12th IMEKO TC1 & TC7 Joint Symposium on
Man, Science & Measurement
September, 3 – 5, 2008, Annecy, France

MATHEMATICAL MODELLING OF HUMAN BRAIN FOR MAGNETIC FIELD TOMOGRAPHY BASED ON MAGNETOENCEPHALOGRAPHY

Sanowar H. Khan[1], *Kirill Y. Aristovich*[1,2], *Alexey I. Borovkov*[2]

[1] Measurement and Instrumentation Centre, City University London, UK, s.h.khan@city.ac.uk
[1] Measurement and Instrumentation Centre, City University London UK, kirill.aristovich.1@city.ac.uk
[2] St. Petersburg State Polytechnic University, St. Petersburg, Russia, borovkov@compmechlab.com

Abstract: This paper presents the methodology and some of the results of mathematical modelling of human brain in magnetic field tomography (MFT) by which sources of tiny bioelectric currents in the brain are located by measuring the magnetic field distribution produced by these current outside the head.

Keywords: Magnetic field tomography, biomedical imaging, magnetoencephalography (MEG).

1. INTRODUCTION

The term magnetic field tomography (MFT) refers to a relatively new imaging modality which involves the localization and subsequent imaging of active areas in the brain by measuring the extremely weak neuromagnetic fields (10–100 fT) produced by neural currents in these areas associated with cognitive processing (magnetoencephalogram). This approach, called the magnetoencephalography (MEG) technique (recording of magnetic fields produced by electrical activity in the brain) is the only truly noninvasive method which could provide information about functional brain activity. The MFT based on MEG data would provide images of the brain 'at work' and as such could have major implications for neurology and neuropsychiatry, in general and new instrumentation for diagnosis, in particular.

Compared to other imaging modalities (e.g. CT, PET, SPECT, MRI), the MEG technique is the only imaging modality that combines high temporal with high spatial resolution. Like any other tomographic technique, MFT involves the solution of two distinct problems: the forward problem of calculating the magnetic field distribution from known generators (sources) in the brain, and the inverse problem of localizing and imaging the generators using MEG data measured around the head, and the data obtained from the forward solution. Besides, an accurate solution of the forward problem has implications for the design, configuration and placement of SQUID sensors, used to measure the neuromagnetic fields around the head, and which constitute the sensing subsystem of the MFT system.

Thus the successful solution of the inverse problem and hence the effectiveness of the MFT as a whole is very much dependent upon the accurate solution of the forward problem. This paper presents an accurate solution of the forward problem using realistic brain geometry and inhomogeneous material properties coupled with various realistic source current approximations. Following from some of the previous works in this area reported, for example in [1-3], the 3D finite element (FE) model of the brain incorporates considerable flexibility in the source current approximation in terms of size, orientation, placement and spatial distribution.

2. FINITE ELEMENT MODELLING OF MAGNETIC FIELDS IN MAGNETOENCEPHALOGRAPHY

2.1 Mathematical Model

The mathematical model of magnetic fields produced by bioelectric current sources in the brain is based on a set of quasistatic Maxwell's equations which lead to an appropriate Poissons's equation. In doing so it is assumed that the permeability of brain matter is the same as that of free space ($\mu=\mu_0$). The quasistatic nature of the field is justified by the fact that bioelectrical activities that give rise to magnetic fields are predominantly of low frequency (from below 100 Hz to less than 1 kHz). This together with the material properties of brain matter (e.g. conductivity σ and permittivity ε) suggest that in calculating the electric field intensity E and magnetic flux density B vectors, the time derivative terms $\partial E/\partial t$ and $\partial B/\partial t$ in Maxwell's equations can be ignored [4]. This leads to the following set of Maxwell's equations:

$$\nabla \times \boldsymbol{B} = \mu_0 \boldsymbol{J} \tag{1}$$

$$\nabla \cdot \boldsymbol{B} = 0 \tag{2}$$

$$\nabla \times \boldsymbol{E} = 0 \tag{3}$$

In (1) above, the total current density

$$\boldsymbol{J} = \boldsymbol{J}_p + \boldsymbol{J}_v = \boldsymbol{J}_p + \sigma \boldsymbol{E} = \boldsymbol{J}_p - \sigma \nabla \varphi, \tag{4}$$

where $\boldsymbol{J}_p$ is the primary 'excitation' current (or impressed current if at the cellular level) produced by electromotive force in the conducting brain tissue. The volume current

$\boldsymbol{J}_v=\sigma\boldsymbol{E}$ is attributed to the effect of macroscopic electric field $\boldsymbol{E}$ on charge carriers [4]. It has been shown that for a realistic brain model with inhomogeneous conductivity distribution, the magnetic field from this volume current can be comparable with that from the primary current source (e.g. dipole) [5]. Thus, the total current density becomes

$$\boldsymbol{J} = \boldsymbol{J}_p + \sigma\boldsymbol{E} = \boldsymbol{J}_p - \sigma\nabla\varphi\,, \tag{5}$$

where φ is the electric scalar potential. The above equations lead to the following Poisson's equation for the quasistatic magnetic field, the solution of which constitutes the solution of the forward problem in magnetic field tomography based on MEG [4]:

$$\nabla\cdot(\sigma\nabla\varphi) = \nabla\boldsymbol{J}_p \text{ in } \Omega=\Omega(x, y, z) \tag{6}$$

Under appropriate boundary conditions (6) is solved for the unknown potential distribution $\varphi=\varphi(x, y, z)$ by finite element method (FEM). The magnetic field $\boldsymbol{B}(\mathbf{r})$ at a given point $\mathbf{r}$ in the problem domain Ω is then found by using

$$\boldsymbol{B}(\mathbf{r}) = \boldsymbol{B}_0(\mathbf{r}) - \frac{\mu_0}{4\pi}\sum_{i=1}^{m}\sigma_i\int_{G_i}\nabla'\varphi\times\frac{\mathbf{R}}{R^3}dv'\,, \tag{7}$$

$$\boldsymbol{B}_0(\mathbf{r}) = \frac{\mu_0}{4\pi}\sum_{i=1}^{m}\int_{G}\boldsymbol{J}_p(\mathbf{r}')\times\frac{\mathbf{R}}{R^3}dv'\,, \tag{8}$$

where the source conductor consists of G_i piecewise homogenous parts, $\boldsymbol{B}_0(\mathbf{r})$ is the magnetic field produced only by the primary current $\boldsymbol{J}_p$, $\mathbf{R}=\mathbf{r}-\mathbf{r}'$ and $\mathbf{r}'$ relates to source regions.

2.1 Realization of 3D Finite Element Model of the Brain

Considering the implications of the accuracy and quality of the solution of forward problem on the solution of the inverse problem in MEG, considerable emphasis was put in this work on the creation of an accurate realistic geometry and realistic material-property brain model. It is believed that this constitutes the strength of this work compared to those carried out previously.

The accurate 3D model was constructed from 150 cross-sectional MRI slices of the brain (which are just 2 mm apart). For each of these slices special graphics editing tools were used to detect accurately edges (isolines) of white and grey matters and filter the isolines. These slices were then stacked vertically and lofted before external bounding surfaces of matters were created using NURBS (non-uniform rational B-spline). Typically, this would, for example create over 30000 NURBS surfaces for the white matter which very accurately represent its intricate geometric features. These also give added flexibility in the FE models to easily take into account differences in brain geometry that may be encountered in realistic geometry brain models. Figs. 1-2 show schematic representations of the process described above.

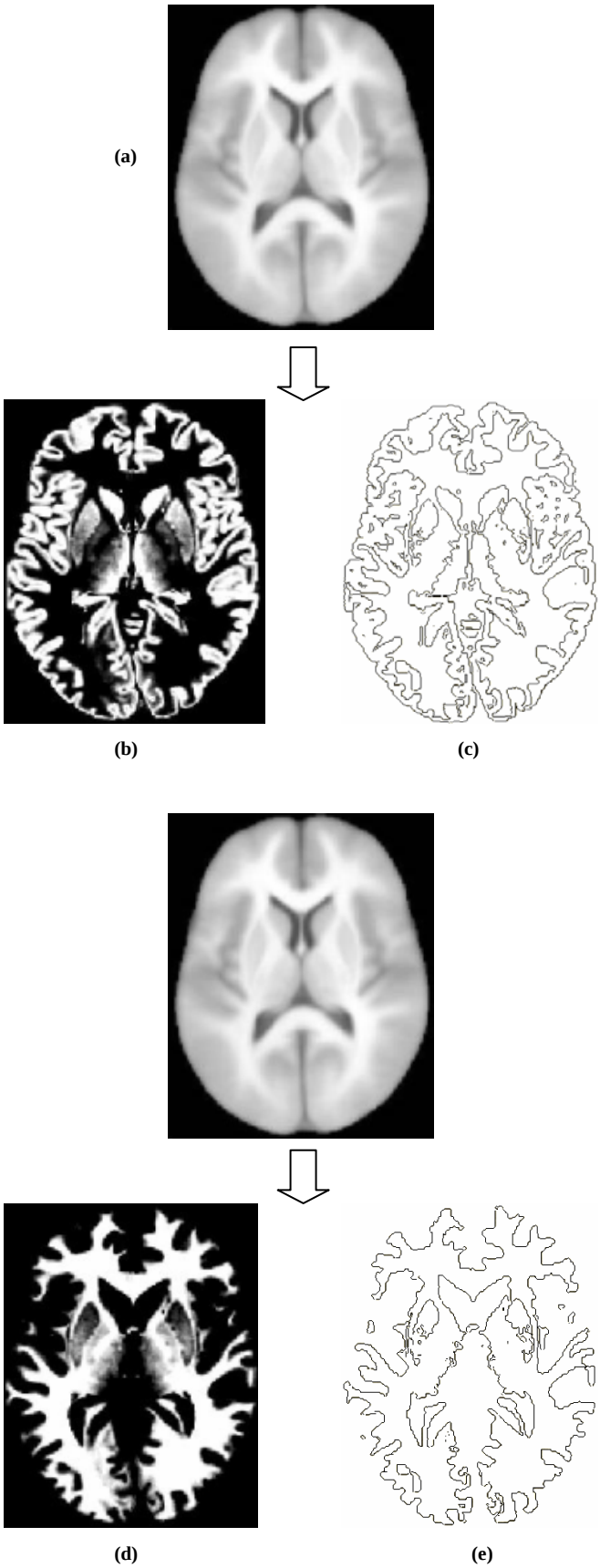

Fig. 1. Preparation of cross-sectional MRI slices (altogether 150, 2 mm-apart slices were used) to build a 3D solid model: (a) typical MRI slice, (b) accurate detection of the edges of grey matter and (c) its resulting isolines; (d) accurate detection of the edges of white matter and (e) its resulting isolines.

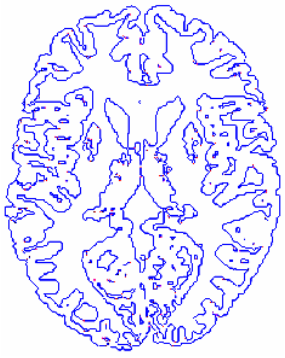

(a)

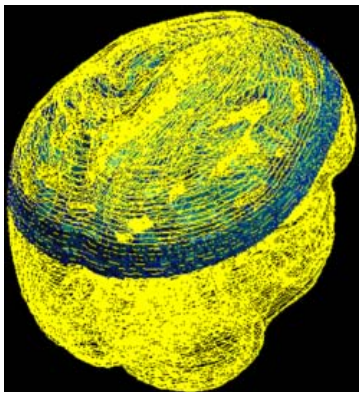

(b)

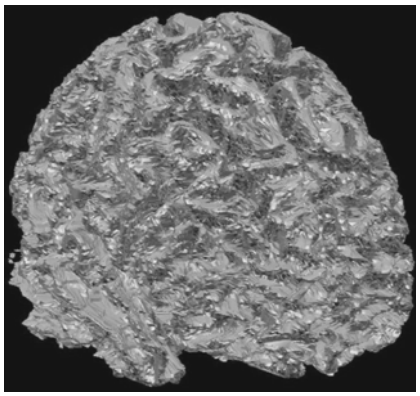

(c)

Fig. 2. Preparation of cross-sectional MRI slices to build a 3D solid model: (a) 'extrusion' of isolines in the 3rd dimension (vertically in the z-direction), (b) 150 edge detected MRI slices stacked vertically before lofting, (c) lofted and NURBS surfaced stack of white matter containing 31000 surfaces.

The complex poly-surfaces (shown in Figs. 3(a) and (b)) obtained above by NURBS surfacing are further smoothed and, if required the number of surfaces is reduced by merging together several surfaces. This is then followed by connecting these surfaces to relevant solid objects. The grey and white matters with 3D polygonal meshes are then combined together by a solid modeller to obtain the 3D solid model of the brain shown in Fig. 3(c). It has been found that the large number of poly-surfaces of which this solid model is made of can pose substantial problems in exporting these data (solid model) to an electromagnetic solver which may have limitations in manipulating such models. It is, therefore recommended that the number of these surfaces should be minimized without compromising the accuracy of geometric and material representations.

(a)

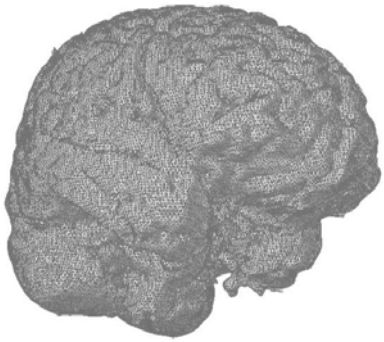

(b)

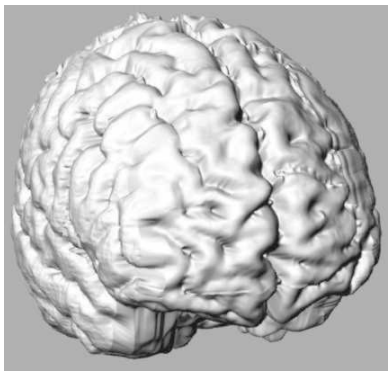

(c)

Fig. 3. Further processing of lofted and NURBS surfaced stack of MRI slices to obtain a 3D solid model before subsequent finite element discretization: (a) 3D polygonal NURBS surfaces for white and (b) grey matter; (c) resulting solid model of the grey matter after smoothing, reduction and merging of poly-surfaces (640 surfaces).

The solid model of the brain obtained above is appropriately discretized taking into account complex nature of the brain geometry, solution accuracy needed and the available computer hardware for field solution. The resulting 3D FE model of the brain used in this work is shown in Fig. 4. A cubic air region, placed sufficiently far away from the brain itself was used to represent the total problem domain (Fig. 4(a)). Zero boundary condition was used on all the surfaces of this cube. For the 3D FE mesh shown in Figs. 4(b) and (c), tetrahedral FE elements with good aspect ratio and regularity were used to represent the brain geometry and physical properties as accurately as it was practicable.

Table 1 shows some of the main parameters of a typical model used in this work. The seemingly large number of elements (over 1.35 million) shown is typically required to take into account accurately various internal and surface geometric features of a human brain.

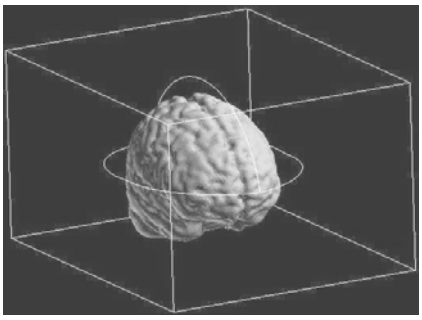

(a)

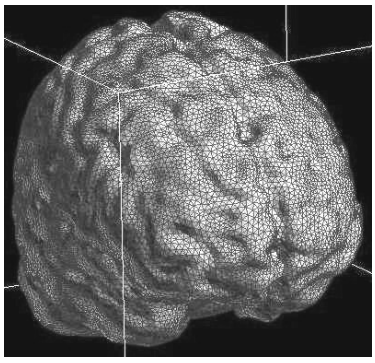

(b)

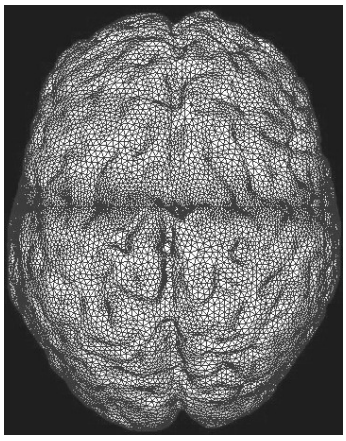

(c)

Fig. 4. Full 3D realistic geometry and realistic material-property brain model: (a) brain model within the problem domain containing 3D surrounding air region; (b), (c) details of FE mesh used.

Table 1. Model parameters

Parameters	Values
Number of elements	1351692
Number of nodes	274993
Type of elements	Tetrahedral
Material properties	Piecewise homogeneous and anisotropic conductivities Permeability – air
Source approximation	Various
Solution type	Quasistatic, linear
Typical solution time	15 min (Intel core2duo, 2.2 GHz, 3.2 GB RAM

3. SOME RESULTS AND DISCUSSION

Fig. 5 shows some of the modelling results which were particularly used to validate the accuracy and flexibility of the realistic geometry and realistic material-property brain model developed in this work. An imaginary 'sensor surface' was used above the head (Fig. 5(a)) on which some of the modelling results were plotted and compared with known analytical solutions for given source configurations. Two examples of such solutions are shown in Figs. 5(b) and (c).

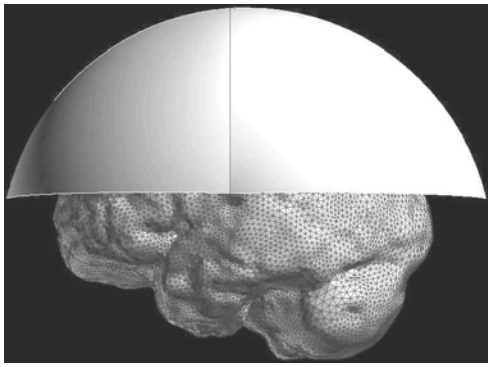

(a)

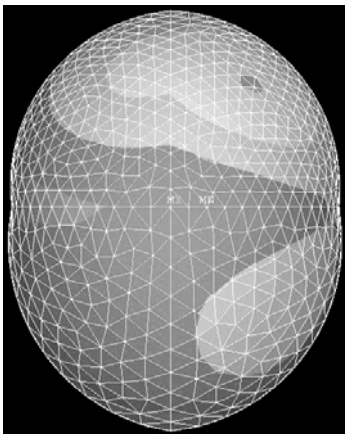

(b)

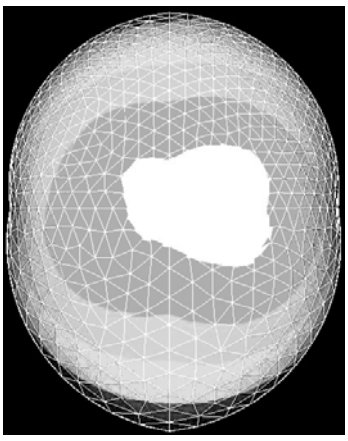

(c)

Fig. 5. Some of the initial results: (a) 3D brain model with imaginary 'sensor surface' above the head on which some of the modelling results were plotted for comparison and validation purposes; (b) magnetic field distribution for a current loop placed vertically and (c) horizontally near the centre of the brain.

These figures show the magnetic field distributions for a circular current loop placed near the center of the brain. The magnitude and the distribution of the field are in good agreement with known solution for such configurations. These and other modelling results confirm the accuracy and, to some extent, the flexibility of the brain model developed.

4. CONCLUSIONS

It is believed that this paper presents the most accurate 3D realistic finite element model of the brain developed so far for solving the forward problem in magnetic field tomography (MFT) brain imaging based on magnetoencephalography (MEG). With over 1.3 million finite elements (extendable up to 5 million), this model provides flexibility in representing the complex internal features and surface topology of the human brain as well as its material inhomogeneity. It can also accommodate, with relative ease any primary source conductor configurations both in terms of its geometry and material properties. This gives considerable flexibility in the solution of the forward problem in MEG which is difficult to achieve using many existing models.

To solve the forward problem in MFT, in this work only the main body of the brain, in which the flow of biomagnetic currents take place during cognitive processing was taken into account. Hence, the skull and other 'non-brain' matters within the skull were justifiably ignored for modelling purposes.

ACKNOWLEDGEMENT

The authors would like to thank the Department for Innovation, Universities and Skills (DIUS), UK and British Council for funding this work under a BRIDGE (British Degrees in Russia) Research Cooperation Grant between City University London and St Petersburg State Polytechnic University, St Petersburg, Russia.

REFERENCES

[1] N. von Ellenrieder, C. H. Muravchik, and A. Nehorai, "MEG forward problem formulation using equivalent surface current densities," *IEEE Transactions on Biomedical Engineering*, vol. 52, Issue 7, pp. 1210-1217, July 2005.

[2] D-H. Kim, C. Won, and G. E. Georghiou, "Assessment of the sensitivity to field localization of various parameters during transcranial magnetic stimulation," *IEEE Transactions on Magnetics*, vol. 43, no. 11, pp. 4016-4022, November 2007.

[3] C. H. Wolters, A. Anwander, X. Tricoche, D. Weinstein, M. A. Koch, and R. S. MacLeod, "Influence of tissue conductivity anisotropy on EEG/MEG field and return current computation in a realistic head model: a simulation and visualization study using high-resolution finite element modeling," *NeuroImage*, vol. 30, pp. 813-826, 2006.

[4] M. Hamalainen, R. Hari, R. J. Ilmoniemi, J. Knuutila, and O. V. Lounasmaa, "Magnetoencephalography-theory, instrumentation, and applications to noninvasive studies of the working human brain," *Reviews of Modern Physics*, vol. 65, no. 2, pp. 413-497, 1993.

[5] R. V. Uitert, D. Weinstein, and C. Johnson, "Volume currents in forward and inverse magnetoencephalographic simulations using realistic head models," *Annals of Biomedical Engineering*, vol. 31, pp. 21-31, 2003.